Coherent spin dynamics of exciton-polaritons in diluted magnetic microcavities

A. Brunetti, M. Vladimirova, and D. Scalbert
Groupe d'Etude des Semi-conducteurs, UMR 5650 CNRS-Université Montpellier 2, Place Eugène Bataillon, 34095 Montpellier Cedex, France

R. André
LSP/CNRS, Université J. Fourier, Grenoble, BP 87, 38402 St Martin d'Héres, France

D. Solnyshkov and G. Malpuech
LASMEA, Blaise Pascal University, 24, av. Des Landais, Aubiere, cedex, France

I. A. Shelykh and A. V. Kavokin
Physics and Astronomy School, University of Southampton, Highfield, Southampton, SO17 1BJ, United Kingdom
(Received 9 February 2006; published 22 May 2006)

Kerr rotation induced by femtosecond pulses in a CdMnTe quantum well embedded in a microcavity is studied under an in-plane magnetic field. Due to giant Zeeman splitting in the diluted magnetic quantum well, in this system we deal with two spin splitted exiton states coupled to the cavity mode. For such a microcavity operating in the strong coupling regime, the polariton spin beats in the time-resolved Kerr rotation signal can be expected at three distinct frequencies. Two of them are observed in our experiments, in a excellent agreement with the theoretical calculation in the framework of the polariton spin density matrix, which accounts for the finite lifetimes of exciton and photon states.

DOI: 10.1103/PhysRevB.73.205337 PACS number(s): 78.47.+p, 71.36.+c, 75.50.Pp

I. INTRODUCTION

Time-resolved Kerr rotation (TRKR) is a pump probe technique appropriate for probing the spin dynamics of carriers and excitons in semiconductors. The angle of Kerr rotation is directly proportional to the projection of the spin polarization vector on the probe beam propagation direction.[1–3] By changing the delay between pump and probe pulses one monitors the spin dynamics of excitons with a subpicosecond resolution. The method has been proven to be extremely successful in measuring both coherent spin evolution and spin dephasing time for electrons, holes, and excitons in semiconductors. In diluted magnetic semiconductors (DMS), TRKR not only provides the information on spin dynamics but also gives direct access to the precession of magnetic ion spins mediated by their interaction with free carriers.[4,5] In this work we apply the TRKR technique in Voigt configuration to study spin dynamics of exciton-polaritons in the $Cd_{0.95}Mn_{0.05}Te$ quantum well (QW) embedded in the CdMgTe/CdMnTe microcavity. Semiconductor microcavities have already been shown to enhance resonantly the Kerr and Faraday effects.[6] Recently, the experimental study of TRKR from a microcavity in the weak coupling regime has been reported in Ref. 7. Here we are interested in the effect of strong coupling between excitons and photons in the cavity and formation of complex quasiparticles, called exciton polaritons.[8] We introduce the spin polarization into a system of cavity polaritons by the circularly polarized pump pulse and probe it, measuring rotation of the polarization plane of the linearly polarized probe pulse reflected from the microcavity. The specifics of our system with respect to the cavities studied in Refs. 6 and 7 consists of embedding of a DMS QW in a microcavity and maintaining the strong coupling regime.

In contrast with conventional QW's, the magnetic field induced splittings in DMS QW's are very large. In a Voigt configuration they are mainly given by the exchange interaction between electrons and magnetic ions. For example, for $Cd_{0.95}Mn_{0.05}Te$ QW the spin splitting at saturation is about 15 meV.[9] This is more than enough to mix so-called dark and bright exciton states having the absolute value of total angular momentum projection to the structure axis $J_z=\pm 2$ and $J_z=\pm 1$, respectively. That is why the spectrum of exciton-polaritons can no more be described in the framework of a two coupled oscillator model,[10] but requires taking into account three coupled oscillators, namely two exciton states separated by Zeeman splitting and the cavity mode. In the TRKR the splittings of these three states determine the frequencies of the oscillations due to precession of the spin polarization coherently excited by the pump pulse around the in-plane magnetic field. Obviously, the giant Zeeman splitting provides a powerful tool to control the coupling between excitons and photons, since excitonic resonances can be tuned in a broad energy band by applying a magnetic field.[11] Similarly, the giant Zeeman effect was used in a CdMnTe cavity to tune the cavity mode by a magnetic field.[12] We show in this paper that polariton formation in the microcavity gives rise to the oscillations in the spin polarization at the frequencies given by polariton splittings under an in-plane magnetic field. An intricate polariton spin dynamics resulting from a combination of Rabi oscillations and exciton spin beats is measured in TRKR experiments and interpreted as a spin polarization transfer between the photon mode and two exciton modes of our system.

The paper is organized as follows. In the next two sections we present the three coupled oscillators model (Sec. II) and more sophisticated polariton spin density matrix approach (Sec. III), which allows us to describe the TRKR

from a DMS QW microcavity, taking into account the decay time of polariton states. The theoretical part is followed by the description of the sample and its CW spectra (Sec. IV), while Sec. V is devoted to the TRKR experiments and a comparison with theoretical results. In the last section we conclude the paper and suggest further experiments.

II. THREE-COUPLED OSCILLATORS MODEL

The eigenenergies of microcavity polaritons can be found by diagonalization of the following Hamiltonian:

$$H_P = H_X + H_C + H_{C-X}, \tag{1}$$

where H_C describes the circularly polarized cavity modes, H_X is the exciton Hamiltonian, and H_{C-X} describes the coupling of photon and exciton states, characterized by the Rabi energy Δ_R. In the exciton Hamiltonian we consider only the heavy hole (hh) exciton and neglect the field induced mixing with the light hole (lh) states and electron hole exchange interaction.[13] The effect of the $hh-lh$ mixing on the TRKR signal has been considered by some of the present authors in Ref. 14. Under these assumptions, $H_X = N_0\alpha x_{eff} s_x < S_x >$, where $< S_x > = \frac{5}{2} B_{5/2}$ is the average spin polarization of Mn ions, s_x is the electron spin projection on the field direction, $N_0\alpha$ is the electron exchange integral, x_{eff} is the effective Mn ions concentration, $B_{5/2}$ is the modified Brillouin function for the Mn spin S=5/2.[9] In general, one should consider the basis including four exciton states with the total angular momenta $J_z = \pm 1$, $J_z = \pm 2$ and two circularly polarized photon states $\sigma^{\pm}$. However, since we neglect the $hh-lh$ mixing, the in-plane magnetic field does not couple $J_z > 0$ and $J_z < 0$ excitons. One can thus consider $J_z > 0$ and σ^+ photon states being completely decoupled from σ^- photon and $J_z < 0$ exciton states. Therefore, for the incident light of a given circular polarization, the basis can be reduced to three states, which we denote as $|ph>$(photon), $|ex>$(bright exciton), $|d>$(dark exciton). The diagonalization of this 3×3 Hamiltonian yields the evolution of three polariton modes under the in-plane magnetic field. These modes will be referred to as photon (P), bright exciton (B), and dark exciton-like (D) polariton modes, while at the nonzero magnetic field each of them contains contributions from three original pure states. The eigenenergies of the three modes are calculated as a function of the magnetic field, as Fig. 1(a), shows. We have used the following set of parameters: $\Delta_R = 8$ meV, zero field detuning between the photon and the exciton modes $\delta = -8.0$ meV, $N_0\alpha = 0.22$ eV, $x_{eff} = 0.04$, $T_{eff} = 5$ K is the effective temperature, accounting for the antiferromagnetic interactions between Mn ions.[15] These parameters are chosen to meet experimental conditions and the sample characteristics, described in the following sections.

A subpicosecond light pulse creates a coherent superposition of the three polariton states (cf. Fig. 2(b)). Since the Kerr rotation signal is governed by the correlation between populations of these states, it is convenient to model the TRKR in the framework of the polariton spin density matrix formalism. The procedure we use to calculate the TRKR and fit the experimental data is described in the next section. Here we calculate analytically the frequencies of the Kerr

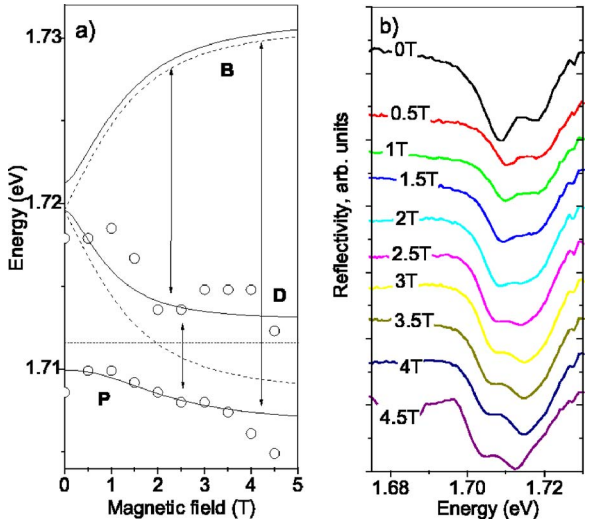

FIG. 1. (Color online) (a) Field dependence of the polariton energies, calculated (solid lines) and extracted from the CW reflectivity spectra. Dashed lines indicate the energies of the noninteracting excitons and photons. Arrows point to the possible polariton transitions. (b) A set of the reflectivity spectra obtained in a Voigt configuration.

oscillations in the system in the simplest three-coupled oscillator model. The wavefunction of each polariton state can be represented as a linear combination of the bare photon, bright exciton, and dark exciton states $\psi_k = a_k|ph> + b_k|ex> + c_k|d>$, where a_k, b_k, c_k are constants. The angle of the Kerr rotation at pump-probe delay Δt is proportional to the average exciton spin polarization in the direction of light propagation:

$$S_z(\Delta t) = \sum_{k,k'} a_k a_{k'} (c_k c_{k'} - b_k b_{k'}) \cos[(\omega_k - \omega_{k'})\Delta t], \tag{2}$$

where $\omega_{k,k'}$ are eigenfrequencies of the polariton states $k,k' = P,B,D$. This means that at a given magnetic field the

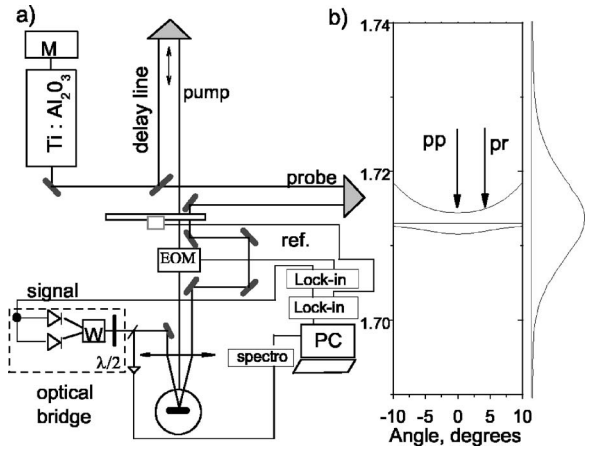

FIG. 2. (a) Experimental set up used for time resolved Kerr rotation experiments. (b) Polariton dispersion at $B = 0$ compared with the spectral shape of the laser pulse, arrows indicate pump and probe incidence angles.

signal may exhibit oscillations at three frequencies given by the splittings between three polariton eigenenergies, in general. These frequencies are shown schematically by arrows in Fig. 1(a). At a zero field, the dark exciton state is not excited by the light, and the eigenvalue problem is reduced to the standard two oscillator model. In this case one should expect the beats only between B and P modes, that is at the vacuum Rabi frequency. These oscillations correspond to the polarization transfer between exciton ($S_z \neq 0$) and photon ($S_z=0$) in the cavity. At a low magnetic field the excitonic states are just slightly mixed, the lower excitonic state ($J_z=2$) is essentially "dark," and the amplitude of the oscillations between P and D states is vanishing, while two other frequencies are expected to show up. In the presence of magnetic field the excitonic states become strongly split, and therefore the bunch of three frequencies may appear.

As will be shown in Sec. V, only two of three frequencies given by the previous simple model could be observed experimentally in the TRKR spectra of our sample. This is partly due to the strong broadening of the polariton modes, which rapidly destroys correlations between some eigenstates making difficult detection of the corresponding eigenfrequencies in the time domain. Since the finite lifetime of the polariton modes and processes of inelastic electron and hole spin relaxation cannot be self-consistently accounted for within the analytical three state model we apply the polariton spin density matrix formalism to fit the experimental data.

III. POLARITON SPIN DENSITY MATRIX FORMALISM

Let us write the model Hamiltonian of the considered system in the second quantization representation,

$$H = H_0 + H_{int} + H_R. \tag{3}$$

The first term describes the coupling of excitons and photons inside the cavity, the second term accounts for the exciton-exciton interactions in the QW, and the third term describes coupling of the cavity photons with the continuum of external photonic modes and coupling of the excitons with the bath of acoustic phonons.

The exciton-photon interaction term reads as

$$\begin{aligned} H_0 = [&\varepsilon_{ex}(a^+_{ex\uparrow}a_{ex\uparrow} + a^+_{ex\downarrow}a_{ex\downarrow}) + \varepsilon_{ph}(a^+_{ph\uparrow}a_{ph\uparrow} + a^+_{ph\downarrow}a_{ph\downarrow}) \\ &+ \varepsilon_D(a^+_{d\uparrow}a_{d\uparrow} + a^+_{d\downarrow}a_{d\downarrow}) + \Delta_R/2(a^+_{ex\uparrow}a_{ph\uparrow} + a^+_{ex\downarrow}a_{ph\downarrow}) \\ &+ \alpha_e(a^+_{ex\uparrow}a_{d\uparrow} + a_{ex\downarrow}a^+_{d\downarrow}) + \alpha_h(a^+_{ex\uparrow}a_{d\downarrow} + a_{ex\downarrow}a^+_{d\uparrow})] + \text{H.c.}, \end{aligned} \tag{4}$$

where we keep the notation used in the previous section for photon and two exciton states (ph, ex, d). The first three terms in Eq. (4) describe the free particles, the fourth is the exciton-photon coupling term, the last two terms correspond to the magnetic field induced mixing of the bright and dark exciton states. The mixing constants are given by

$$\alpha_{e,h} = g_{e,h}\mu_B B_{eff} \tag{5}$$

where $g_{e,h}$ is an electron/hole g factor, B_{eff} is a sum of the external magnetic field B and exchange magnetic field B_{exch} created by the Mn^{2+} ions. As in the previous section we shall neglect the field-induced *hh-lh* mixing and thus we shall suppose $g_h=0$. The exchange field is given by the following expression:

$$B_{exch} = \frac{N_0\alpha_e x_{eff}\langle S_x\rangle}{g_e\mu_B}. \tag{6}$$

The exciton-exciton interactions are essential for the photo-induced Kerr rotation and the corresponding term of the Hamiltonian reads as

$$\begin{aligned} H_{int} = &\frac{\beta_{ex-ex,\uparrow\uparrow}}{2}(a^+_{ex\uparrow}a_{ex\uparrow}a^+_{ex\uparrow}a_{ex\uparrow} + a^+_{ex\downarrow}a_{ex\downarrow}a^+_{ex\downarrow}a_{ex\downarrow}) \\ &+ \beta_{ex-ex,\uparrow\downarrow}(a^+_{ex\uparrow}a_{ex\uparrow}a^+_{ex\downarrow}a_{ex\downarrow}) + \frac{\beta_{d-d,\uparrow\uparrow}}{2}(a^+_{d\uparrow}a_{d\uparrow}a^+_{d\uparrow}a_{d\uparrow} \\ &+ a^+_{d\downarrow}a_{d\downarrow}a^+_{d\downarrow}a_{d\downarrow}) + \beta_{d-d,\uparrow\downarrow}(a^+_{d\uparrow}a_{d\uparrow}a^+_{d\downarrow}a_{d\downarrow}) \\ &+ \beta_{ex-d,\uparrow\uparrow}(a^+_{ex\uparrow}a_{ex\uparrow}a^+_{d\uparrow}a_{d\uparrow} + a^+_{ex\downarrow}a_{ex\downarrow}a^+_{d\downarrow}a_{d\downarrow}) \\ &+ \beta_{ex-d,\uparrow\downarrow}(a^+_{ex\uparrow}a_{ex\uparrow}a^+_{d\downarrow}a_{d\downarrow} + a^+_{d\uparrow}a_{d\uparrow}a^+_{ex\downarrow}a_{ex\downarrow}) \end{aligned} \tag{7}$$

where the matrix elements $\beta_{ex-ex,k}$, $\beta_{d-d,k}$, and $\beta_{ex-d,k}$ correspond to the interactions between bright excitons, dark excitons, and mutual bright exciton-dark exciton interactions, respectively. The indices $k=\uparrow\uparrow, \downarrow\uparrow$ stand for the mutual orientations of the interacting exciton spins. For the description of Kerr rotation it is sufficient to retain only the term corresponding to the interactions of bright excitons treated in the mean-field approximation.[16] Neglecting all other terms, the exciton-exciton interaction Hamiltonian reads as

$$H_{int} = (\beta_1 N_{ex\uparrow} + \beta_2 N_{ex\downarrow})a^+_{ex\uparrow}a_{ex\uparrow} + (\beta_1 N_{ex\downarrow} + \beta_2 N_{ex\uparrow})a^+_{ex\downarrow}a_{ex\downarrow}, \tag{8}$$

where $N_{ex\uparrow}$, $N_{ex\downarrow}$ are the occupation numbers of spin-up and spin-down exciton states. In microcavities, interactions between excitons with parallel spin projections on the structure growth axis is much stronger than for the excitons with antiparallel spin projections, $\beta_1 \gg \beta_2$.[17] In the case when the excitonic system has nonzero circular polarization this results in the appearance of the concentration dependent magnetic field directed along the z axis, which induces the Kerr rotation of the linear components of the polarization.[18] The constant β_1 is approximately given by[19]

$$\beta_1 = \frac{6a_B^2 E_b}{S}, \tag{9}$$

where a_B is the exciton Bohr radius, E_b is the exciton binding energy, and S is an area of the laser spot.

Finally, the term H_R describes interactions of the cavity mode with the external continuum of photons and coupling of excitons with the acoustic phonon bath. It reads as

$$H_R = \sum_{\omega} C_{\omega}(a^+_{ph\uparrow}c_{\omega\uparrow} + a^+_{ph\downarrow}c_{\omega\downarrow}) + \sum_{\omega} B_{\omega}b_{\omega}(a^+_{ex\downarrow} + a^+_{ex\uparrow}t) + \sum_{\omega} [Q_{\omega,e}(b_{\omega} + b^+_{\omega})(a_{ex\uparrow}a^+_{d\uparrow} + a_{ex\downarrow}a^+_{d\downarrow})] + \sum_{\omega} [Q_{\omega,h}(b_{\omega} + b^+_{\omega})(a_{ex\uparrow}a^+_{d\downarrow} + a_{ex\downarrow}a^+_{d\uparrow})] + \text{H.c.}, \quad (10)$$

where $c_{\omega\uparrow,\downarrow}$ are annihilation operators of the right and left circular polarized external photons, b_{ω} is th annihilation operator of the phonon. The first two terms stand for the transitions between the cavity mode and external photons and between excitons and acoustic phonons. They are characterized by the coupling constants C_{ω} and B_{ω}. The last two terms describe the phonon-assisted spin flips of electrons and holes, leading to their spin relaxation. Generally, H_R corresponds to the coupling of the quantum system with a classical reservoir, and can be treated within the framework of the Born-Markov approximation, familiar in the quantum optics.[20] It results in the semiclassical terms describing the finite lifetimes of the cavity mode and the excitons, the external pumping, and the processes of inelastic spin relaxation.

Polariton dynamics in DMS microcavities can be modeled by the Liouville-von Neumann equation for the density matrix ρ, with additional Lindblad terms describing the finite lifetime of the polariton modes and inelastic processes of the spin relaxation of electrons and holes forming the exciton. The presence of exciton-exciton interactions makes the equation nonlinear, as the Hamiltonian itself depends on the occupation numbers, i.e., on the diagonal elements of the density matrix. In the Born-Markov approximation, the Liouville-von Neumann equation reads as

$$\frac{d\rho}{dt} = \frac{i}{\hbar}[\rho; H_0 + H_{int}(\rho)] + \Gamma\rho + P_{pump} + P_{probe}, \quad (11)$$

where the first term describes the evolution of the system in the external in-plane magnetic field, the second term describes the damping processes such as the radiative decay and spin relaxation of electrons and holes,[21] the last terms describe pump and probe action. In the basis of the four exciton states $J_z = \pm 1$, $J_z = \pm 2$ and two circularly polarized photon states $\sigma^{\pm}$ the diagonal components of the density matrix give the occupation numbers of these 6 states:

$$\rho_{11} = N_{ex\uparrow}, \rho_{22} = N_{ex\downarrow}, \rho_{33} = N_{ph\uparrow}, \rho_{44} = N_{ph\downarrow},$$

$$\rho_{55} = N_{d\uparrow}, \rho_{66} = N_{d\downarrow}.$$

The Hamiltonian $H_0 + H_{int}$ in this basis is given by the matrix

$$\begin{pmatrix} \varepsilon_{ex} + \beta_1\rho_{11} + \beta_2\rho_{22} & 0 & \frac{\Delta_R}{2} & 0 & \alpha_e & 0 \\ 0 & \varepsilon_{ex} + \beta_1\rho_{22} + \beta_2\rho_{11} & 0 & \frac{\Delta_R}{2} & 0 & \alpha_e \\ \frac{\Delta_R}{2} & 0 & \varepsilon_{ph} & 0 & 0 & 0 \\ 0 & \frac{\Delta_R}{2} & 0 & \varepsilon_{ph} & 0 & 0 \\ \alpha_e^* & 0 & 0 & 0 & \varepsilon_d & 0 \\ 0 & \alpha_e^* & 0 & 0 & 0 & \varepsilon_d \end{pmatrix}. \quad (12)$$

The action of the superoperator Γ can be represented in the Linblad form.[20] It is defined in such a way that, once applied to the density matrix, it yields the following matrix elements:

$$(\Gamma\rho)_{11} = (\rho_{55} - \rho_{11})/\tau_{e\perp} + (\rho_{66} - \rho_{11})/\tau_{h\perp},$$

$$(\Gamma\rho)_{22} = (\rho_{66} - \rho_{22})/\tau_{e\perp} + (\rho_{55} - \rho_{22})/\tau_{h\perp},$$

$$(\Gamma\rho)_{33} = -\rho_{33}/\tau_{ph},$$

$$(\Gamma\rho)_{44} = -\rho_{44}/\tau_{ph},$$

$$(\Gamma\rho)_{55} = (\rho_{11} - \rho_{55})/\tau_{e\perp} + (\rho_{22} - \rho_{55})/\tau_{h\perp},$$

$$(\Gamma\rho)_{66} = (\rho_{22} - \rho_{66})/\tau_{e\perp} + (\rho_{11} - \rho_{66})/\tau_{h\perp},$$

$$(\Gamma\rho)_{13,31} = -\frac{1}{2\tau_{ph}}\rho_{13,31}, \quad (\Gamma\rho)_{14,41} = -\frac{1}{2\tau_{ph}}\rho_{14,41},$$

$$(\Gamma\rho)_{23,32} = -\frac{1}{2\tau_{ph}}\rho_{23,32}, \quad (\Gamma\rho)_{24,42} = -\frac{1}{2\tau_{ph}}\rho_{24,42},$$

$$(\Gamma\rho)_{34,43} = -\frac{1}{\tau_{ph}}\rho_{34,43}, \quad (\Gamma\rho)_{35,53} = -\frac{1}{2\tau_{ph}}\rho_{35,53},$$

$$(\Gamma\rho)_{36,63} = -\frac{1}{2\tau_{ph}}\rho_{36,63}, \quad (\Gamma\rho)_{45,54} = -\frac{1}{2\tau_{ph}}\rho_{45,54},$$

$$(\Gamma\rho)_{46,64} = -\frac{1}{2\tau_{ph}}\rho_{46,64}, \quad (\Gamma\rho)_{12,21} = (\Gamma\rho)_{15,51} = (\Gamma\rho)_{16,61} = (\Gamma\rho)_{25,52} = (\Gamma\rho)_{26,62} = (\Gamma\rho)_{56,65} = 0, \quad (13)$$

where τ_e, τ_h are longitudinal spin relaxation times of the electrons and holes, the in-plane spin relaxation of the electrons and holes being neglected, as it has a negligible impact on the magnetization in the z direction and the TRKR signal in our system. We assumed the infinite nonradiative lifetime of the excitonic states, as in reality it is much longer than

both the lifetime of the photon mode and spin relaxation times.

The creation of polaritons by the pump and probe pulses is described by the terms P_{pump} and P_{probe} in Eq. (11). For the circularly polarized pump pulse, all the matrix elements of P_{pump} are zero, except one:

$$P_{pump,33}(t) = A_{pp}^2 * \cos^2(\omega t) * \exp(-t^2/\tau^2). \quad (14)$$

For the linearly polarized probe pulse term, four matrix elements are nonzero:

$$P_{probe,33}(t) = P_{44}(t) = P_{34}(t) = P_{43}(t) = A_{pr}^2/2 * \cos^2[\omega(t-\Delta t)] * \exp[-(t-\Delta t)^2/\tau^2]. \quad (15)$$

Here τ is the duration of the light pulse, ω is the central frequency, and A_{pp}, A_{pr} are amplitudes of the pump and probe electric fields. The linear polarization of the emitted signal as a function of time is governed by the following correlator:

$$S_{ph}(t,\Delta t) = \langle a_{ph\downarrow}^{+} a_{ph\uparrow} \rangle = \rho_{34}^{*}(t,\Delta t). \quad (16)$$

The time-integrated linear polarization of the signal is

$$S_{ph}(\Delta t) = \int_0^\infty \rho_{34}^{*}(t,\Delta t)dt = S_x(\Delta t) + iS_y(\Delta t) \quad (17)$$

Finally, the angle of the Kerr rotation can be calculated as

$$\phi(\Delta t) = \frac{1}{2}\arctan\left(\frac{S_y(\Delta t)}{S_x(\Delta t)}\right), \quad (18)$$

where the factor 1/2 appears because 90° rotation of the polarization of the light corresponds to the 180° rotation of the pseudospin.

IV. SAMPLE AND CW REFLECTIVITY

The sample under study was grown by molecular beam epitaxy on a $Cd_{0.88}Zn_{0.12}Te$ [100] oriented substrate. The back and front Bragg mirrors are formed by 20 and 6.5 pairs of $\lambda/4$-thick $Cd_{0.4}Mg_{0.6}Te/Cd_{0.75}Mn_{0.25}Te$, respectively. The $Cd_{0.95}Mn_{0.05}Te$ QW of 8 nm width is embedded in the middle of $\lambda/2 Cd_{0.4}Mg_{0.6}Te$ cavity. The asymmetric Bragg mirrors were grown to maximize the magneto-optical Kerr rotation in the presence of small magnetic fields, while the high energy gap of the compounds ensures the absence of Kerr effect in the mirrors at the QW exciton resonance.[22] The reflectivity of the mirrors was estimated to be 76% for the top and 98% for the back mirror. The cavity is grown on a wedge (12 meV/mm), which allows to tune the cavity mode by simple shift of the laser spot. Here we only discuss the data obtained at the point corresponding to negative detuning between photon and exciton modes of −8 meV at zero field (i.e. the bare photon mode is 8 meV lower than the bare exciton mode). A set of the reflectivity spectra obtained in the Voigt configuration using circularly polarized light from a tunable CW Ti:sapphire laser is shown in Fig. 1(b). Two anticrossing polariton branches can be distinguished in Fig. 1(b), the exciton-like branch moving across the cavity mode towards lower energies. The corresponding spectral minima are shown in Fig. 1(a). One can see that the anticrossing between lower energy exciton and the photon modes is well reproduced by the model, while the highest energy polariton mode does not appear in the spectra since the upper exciton state shifts significantly with magnetic field. This mode contains a very small photon fraction and is not visible in reflection therefore. Note, that the polariton broadening Γ is about 3 meV which corresponds to the polariton dephasing time of 0.25 ps, while the Rabi splitting $\Delta_R = 8$ meV. In time resolved measurements discussed below, this Rabi splitting is expected to give rise to polariton beats with the frequency $\Omega_R = 1.35$ ps (at the anticrossing point), whereas the polariton dephasing governs the decay time of these beats.

Overall, the strong coupling criterion $\Delta_R/\Gamma > \hbar$ is satisfied in our sample. This is in agreement with the conclusions of M. Haddad *et al.*,[11] who worked with a similar sample in order to demonstrate the enhancement of the Faraday rotation in an asymmetric cavity.

V. TIME-RESOLVED KERR ROTATION EXPERIMENTS

The experimental setup for TRKR experiments is shown in Fig. 2(a). The 120 fs pulses at a 82 MHz repetition rate are delivered by a titanium-sapphire laser pumped by Millenia (SpectraPhysics). The pulse shape was controlled aposteriori by a home-built autocorrelator. The pump and probe beams are separated by a semitransparent plate, and the delay between the pulses is controlled by the mechanical delay line. The helicity of the pump beam is modulated between left and right circular polarizations at 50 kHz using an elastooptical modulator, while both pump and probe intensities are modulated with a double-blade chopper, so that the modulation of the Kerr rotation signal is threefold. In the majority of experiments the total power incident on the sample is about 1 mW, and both beams are focused on the sample with the same 25 cm focal lens producing a spot of about 150 μm diameter, with an angle between pump and probe about 4°. The spectral width of the 120 fs pulses (about 15 meV) is much larger than the Rabi splitting in the sample, therefore both polariton branches are excited and probed simultaneously. Moreover, we can expect that the pump pulse creates polaritons at $k \neq 0$ since the disorder is particularly important in magnetic structures. We do not have, however, experimental proof, that TRKR signal probed at 4° results from the polaritons created by the pump pulse with the same wave vector as those created by the probe pulse, and not from the $k=0$ polaritons. This situation is illustrated in Fig. 2(b), where the polariton dispersion in the sample at a zero field is shown schematically, together with the spectral shape of the laser pulse, while the arrows indicate pump and probe incidence angles.

The probe beam reflected by the sample is directed onto a balanced optical bridge, which yields an electrical signal proportional to the pump-induced Kerr rotation angle. A small part of the reflected probe beam intensity is collected in the optical fiber and used to measure the spectra of the reflected light. The magnetic field is created by a superconductive split

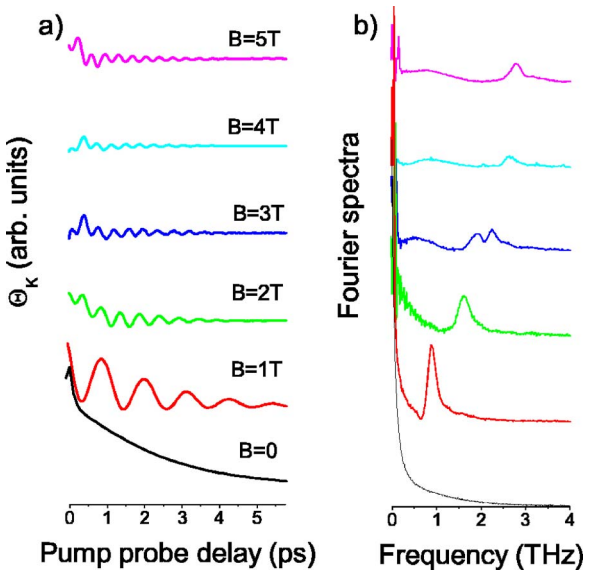

FIG. 3. (Color online) (a) Kerr rotation scans under magnetic field in Voigt configuration. The laser excitation energy is 1.715 eV for $B=0-2$ T, 1.710 eV for $B=3$ T and 1.702 eV for 4–5 T. (b) The corresponding Fourier spectra.

coil, while the sample is placed in the cryostat at $T=2$ K.

Figure 3(a) shows the TRKR scans measured under the in-plane magnetic field from 0 to 5 T. Our main concern in this work is the polariton spin precession, therefore we show here the signal at short pump-probe delays, where it is clearly seen. At longer delays the signal is mainly given by the precession of the Mn^{2+} spins, coherently rotated due to the exchange interaction with the photocreated holes (see Fig. 4 from Ref. 14). In Fig. 3(a), one can see that at a zero field the signal decays exponentially, while in the presence of the field the oscillations show up. Moreover, above 3 T we observe the beats, which is an additional lower frequency arising in the signal. This can be seen in the Fourier spectra of the TRKR signal, Fig. 3(b). The summary of the frequencies observed in the TRKR is reported in Fig. 4 (circles), together with the polariton splittings calculated previously (lines), using the same parameters as in Fig. 1(a).[23] We identify the higher frequency beats as the beats between two

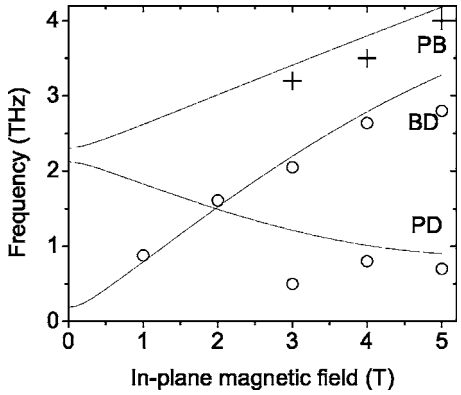

FIG. 4. Polariton beats frequency extracted from the Fourier spectra shown in Fig. 3(b) as a function of the applied magnetic field (circles, crosses). Solid lines show theoretical prediction.

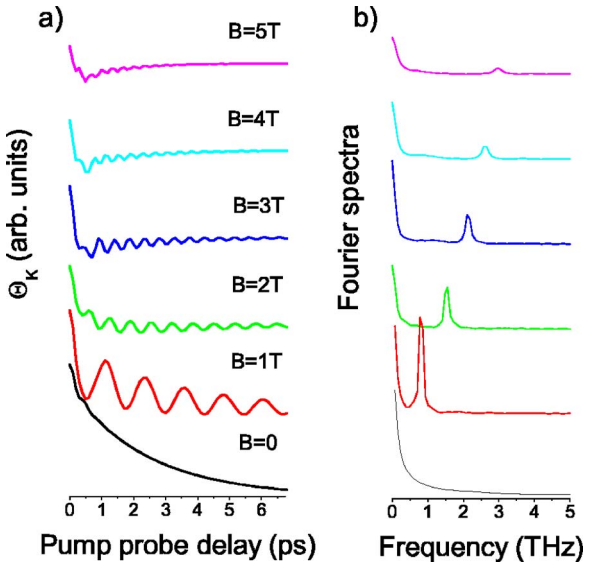

FIG. 5. (Color online) (a) Calculated Kerr rotation scans under magnetic field in Voigt configuration. (b) The corresponding Fourier spectra.

excitonlike polariton branches (*BD*), while the lower frequency beats are between *P* and *D* states (*PD*). One can notice that the peak associated with the exciton spin precession (*BD*) splits at 3 T and has an asymmetric form at higher fields, suggesting exciton spin beats at two different frequencies. We believe that this is a manifestation of the inhomogeneous Mn^{2+} spin heating, an out of equilibrium phenomenon described in Ref. 24.

At zero and low fields the absence of the *PD* beats is not surprising. Indeed, as argued in Sec. II, since the excitonic states are only weakly mixed, the polariton component *D* resulting from the exciton dark state is almost not excited by the incident light. As soon as the magnetic field mixes the exciton states, the *PD* beats arise in the signal. However, neither at high nor at low fields the polariton beats between *P* and *B* branches are clearly observed. At a zero field, the absence of the *PB* beats is particularly evident, since we observe pure exponential decay of the TRKR signal, and neither at high fields the polariton beats between *P* and *B* branches are clearly observed. We explain it by a very short photon lifetime τ_{ph} in our sample. Indeed, from the CW reflectivity measurements it can be estimated as $\tau_{ph}=\hbar/\Gamma=0.25$ ps, where $\Gamma=3$ meV is the polariton broadening. The results of the calculation of the TRKR signal for the experimentally explored range of fields in the framework of the polariton spin density matrix formalism, assuming $\Delta_R=5.2$ meV, $\delta=-8.0$ meV, $T_{\text{eff}}=10$ K, and $\tau=0.25$ ps are shown in Fig. 5.

At zero field, the resonance corresponding to the *PB* beats is hardly visible because it is extremely weak. Its amplitude increases when one either increases the photon lifetime or reduces the detuning between the photon and the exciton mode. To illustrate the effect of the photon lifetime on the amplitude of Rabi oscillations, we show in Fig. 6(a) the results of calculation using $\tau_{ph}=0.5$ ps and 0.2 ps at $B=0$. One can see that the oscillations that are smeared out in the case of $\tau_{ph}=0.2$ ps and can be clearly distinguished when

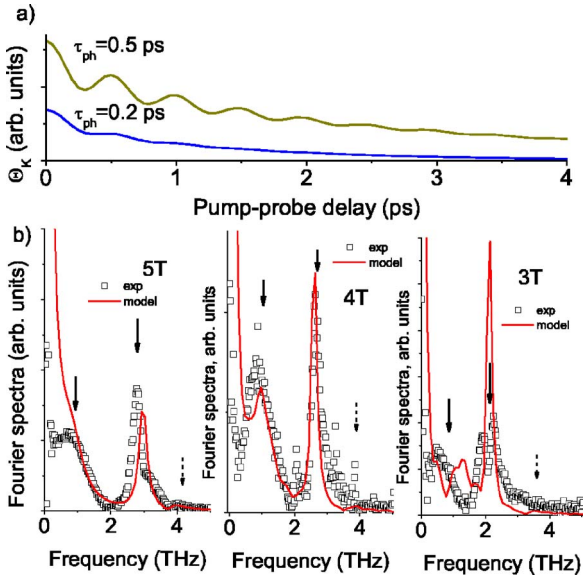

FIG. 6. (Color online) (a) Calculated Kerr rotation scans at $B=0$ and two different values of the photon lifetime. One can observe the smearing of Rabi oscillations when $\tau_{ph}=0.2$ ps. (b) The Fourier spectra obtained from calculated and measured Kerr rotation scans from 3 to 5 T. Arrows indicate the resonance frequencies.

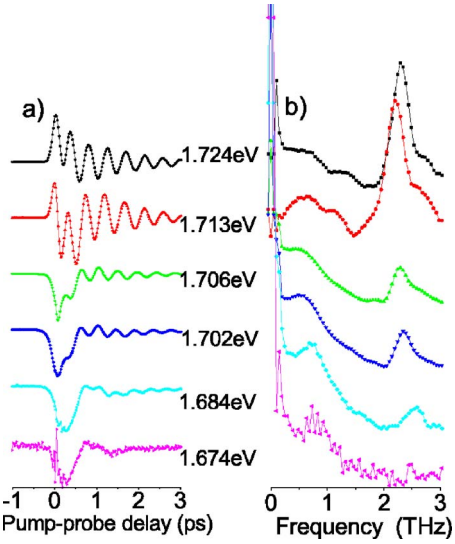

FIG. 7. (Color online) (a) Kerr rotation scans at $B=5$ T and pump and probe energy from 1.674 to 1.724 eV. (b) The corresponding Fourier spectra.

$\tau_{ph}=0.5$ ps. Fig. 6(b) shows in more detail the Fourier spectra of TRKR at 3, 4 and 5 T, together with calculated curves. At high fields, the weak and wide spectral features not well separated from *BD* oscillations peak may be interpreted as rapidly decaying *PB* beats. The corresponding frequencies are shown by crosses in Fig. 4. Thus, under magnetic field three resonances appear in our numerical simulations. However, the *PB* resonance remains extremely weak, so that the calculated signal fits rather well the experimental results.

Since at high field the TRKR contains two contributions (*PD* and *BD*), we could alter the relative excitation of the polariton branches in order to enhance the relative weight of one of them.The resulting experimental spectra are plotted in Fig. 7, where the TRKR scans and their Fourier spectra are shown for different excitation energies. It appears that by lowering the excitation energy untill $E=1.674$ eV, the excitonic (*BD*) contribution can be completely eliminated, while at high excitation energies it dominates the spectra. Remarkably, in the former case, the signal oscillates between negative values and zero. Since the polariton beats can be understood as cycles of absorption and emission of the photon by the exciton, the beats between *P* and *D* polariton branches correspond to the polarization transfer between the photon and "dark" exciton state. When the polariton is in the photon state, $S_z=0$. The observation of negative Kerr rotation values means that when the polariton is in the exciton state, in the most part of time $S_z \neq 0$, which is possible if the exciton spin rotation around the magnetic field is superimposed to the exciton-photon beats. On the other hand, at $E=1.724$ eV, the oscillations are symmetrical with respect to zero angle. In this case, both positive and negative half-periods of the oscillations of S_z contribute to the TRKR signal. Note, however, that in order to obtain a nonzero signal, the excitation should remain resonant with one of the excitonic transitions.

VI. CONCLUSIONS

In conclusion, we have studied the TRKR from the strong coupling CdMnTe quantum well microcavity. We have shown that in the presence of the in-plane magnetic field and at a given circular polarization of light, three polariton eigenstates should be considered. Using the polariton spin density matrix formalism, we propose the procedure, which allows us to calculate the TRKR signal in these conditions. The model is in good agreement with experimental results, which reveal two kinds of polariton beats, namely the beats between two excitonlike polariton branches and between one of the excitonlike states and the photonlike state. Some eigenfrequencies of the system are found to be hidden because of the short cavity photon lifetime and strong negative detuning between cavity and exciton modes. Variation of the excitation energy allows us to enhance or suppress the relative weight of two components of the signal corresponding to exciton-exciton and exciton-photon beats.

The observation of the polariton beats at Rabi frequency, that is, between the photonlike and the most split from the excitonlike state, and the observation of Kerr oscillations without a magnetic field are theoretically possible in microcavities. However, to see such kinds of oscillations, the condition on the photon lifetime should be fulfilled: $\Delta_R * \tau > 2\pi\hbar$. This condition is stronger than the condition for the strong coupling $\Delta_R * \tau > \hbar$, and it is not satisfied in our sample. Therefore, while in CW reflectivity spectra the anticrossing structure typical for the strong coupling regime is observed, in TRKR experiments Rabi oscillations do not emerge. Thus, an observation of the Rabi oscillations in the TRKR requires the sample with a longer photon lifetime, or, in other words, with the Bragg mirrors of higher a quality.

We acknowledge support from the Marie-Curie RTN project 503677 "Clermont2."

[1] J. J. Baumberg, S. A. Crooker, D. D. Awschalom, N. Samarth, H. Luo, and J. K. Furdyna, Phys. Rev. B **50**, 7689 (1994).
[2] J. J. Baumberg, D. D. Awschalom, N. Samarth, H. Luo, and J. K. Furdyna, Phys. Rev. Lett. **72**, 717 (1994).
[3] N. Linder and L. J. Sham, Physica E (Amsterdam) **2**, 412 (1998).
[4] S. A. Crooker, J. J. Baumberg, F. Flack, N. Samarth, and D. D. Awschalom, Phys. Rev. Lett. **77**, 2814 (1996).
[5] D. Scalbert, F. Teppe, M. Vladimirova, S. Tatarenko, J. Cibert, and M. Nawrocki, Phys. Rev. B **70**, 245304 (2004).
[6] A. V. Kavokin, M. R. Vladimirova, M. A. Kaliteevski, O. Lyngnes, J. D. Berger, H. M. Gibbs, and G. Khitrova, Phys. Rev. B **56**, 1087 (1997).
[7] G. Salis, and M. Moser, Phys. Rev. B **72**, 115325 (2005).
[8] A. Kavokin and G. Malpuech, *Cavity Polaritons* (Elsevier, Amsterdam, 2003).
[9] "Diluted magnetic semiconductors," *Semiconductors and Semimetals*, edited by J. K. Furdyna and J. Kossut (Academic, New York, 1988), Vol. 25.
[10] V. Savona, L. C. Andreani, P. Schwendimann, and A. Quattropani, Solid State Commun. **93**, 733 (1995).
[11] M. Haddad, R. André, R. Frey, and C. Flytzanis, Solid State Commun. **111**, 61 (1999).
[12] H. Ulmer-Tuffigo, F. Kany, G. Feuillet, R. Langer, J. Bleuse, and J. L. Pautrat, J. Cryst. Growth **159**, 605 (1996).
[13] The strength of the hh-lh coupling is given by the ratio between the Zeeman splitting of the lh states Δ_Z^{lh}, and *hh-lh* energy splitting $\Delta^{hh\text{-}lh}=50$ meV. In our experimental conditions, $\Delta_Z^{lh}=15$ meV, about one half of its value at saturation of magnetization, and therefore is low enought to neglect the *hh-lh* mixing.
[14] A. Brunetti, M. Vladimirova, D. Scalbert, and R. André, Prog. Solid State Chem. **2**, 3876 (2005).
[15] J. A. Gaj, R. Planel, and G. Fishman, Solid State Commun. **29**, 435 (1979).
[16] Stricktly speaking, we have no other reason to neglect all other interactions, apart from the fact that to describe our experiment it is sufficient to keep only the interactions between bright excitons. But clearly, if we take all possible interactions into account we shall have two additional free parameters and no essential new physics would be brought in.
[17] P. Renucci, T. Amand, X. Marie, P. Senellart, J. Bloch, B. Sermage, and K. V. Kavokin, Phys. Rev. B **72**, 075317 (2005).
[18] I. Shelykh, G. Malpuech, K. V. Kavokin, A. V. Kavokin, and P. Bigenwald, Phys. Rev. B **70**, 115301 (2004).
[19] F. Tassone and Y. Yamamoto, Phys. Rev. B **59**, 10830 (1999).
[20] H. J. Carmichael, *Statistical Methods in Quantum optics. Master Equations and Fokker Planck Equations* (Springer-Verlag, Berlin, 2002).
[21] We have used the compact symbolic form for of the damping term, note, however, Γ, is not a "real" operator acting in the Hilbert space, but a ″superoperator″ whose action can be determined only for the density matrix.
[22] D. Pereda Cubian, M. Haddad, R. André, R. Frey, G. Roosen, J. L. Arce Diego, and C. Flytzanis, Phys. Rev. B **67**, 045308 (2003).
[23] The temperature $T=7$ K was used for the TRKR experiments description instead of $T=2$ K for CW experiments in order to account for the higher excitation level.
[24] F. Teppe, M. Vladimirova, D. Scalbert, T. Wojtowicz, and J. Kossut, Phys. Rev. B **67**, 033304 (2003); M. Vladimirova, D. Scalbert, and C. Misbah, *ibid.* **71**, 233203 (2005).